

AUTOMATED DESIGN OF TISSUE ENGINEERING SCAFFOLDS BY ADVANCED CAD

E. Ramin* and R. A. Harris*

* Rapid Manufacturing Research Group, Wolfson School of Mechanical & Manufacturing Engineering, Loughborough University, UK

Abstract

The design of scaffolds with an intricate and controlled internal structure represents a challenge for Tissue Engineering. Several scaffold manufacturing techniques allow the creation of complex and random architectures, but have little or no control over geometrical parameters such as pore size, shape and interconnectivity- things that are essential for tissue regeneration. The combined use of CAD software and layer manufacturing techniques allow a high degree of control over those parameters, resulting in reproducible geometrical architectures. However, the design of the complex and intricate network of channels that are required in conventional CAD, is extremely time consuming: manually setting thousands of different geometrical parameters may require several days in which to design the individual scaffold structures. This research proposes an automated design methodology in order to overcome those limitations. The combined use of Object Oriented Programming and advanced CAD software, allows the rapid generation of thousands of different geometrical elements. Each has a different set of parameters that can be changed by the software, either randomly or according to a given mathematical formula, so that they match the different distribution of geometrical elements such as pore size and pore interconnectivity.

This work describes a methodology that has been used to design five cubic scaffolds with pore size ranging from about 200 to 800 μm , each with an increased complexity of the internal geometry.

Keywords: Tissue Engineering scaffolds, Automated Design, Advanced CAD Programming, Layer Manufacturing

1. Introduction

The goal of Tissue Engineering (TE) is to "restore function through the delivery of living elements which become integrated into the patient" (Vacanti and Langer, 1999).

Currently, there are two areas of investigation for the physical realisation of TE. The first, termed 'direct organ printing', approaches the direct manufacture of organs and tissues using Layer Manufacturing (LM) methodologies, adapted in order to process biological materials, cells and living tissues (Mironov *et al.*, 2003). It will probably be several years before the direct printing of living tissues becomes a reality.

The second approach consists of producing scaffolds which are latterly seeded with cells. These scaffolds feature macro and micro porosity to promote directed natural tissue regeneration *in vitro*. An alternative approach involves the implantation of scaffolds without cells directly into the defect cavity *in vivo*, to serve as a template for cell and tissue growth (Capito and Spector, 2003).

In vitro tests show that the lack of oxygen and nutrients affects the depth of penetration inside the scaffold, which, for foam structures, is less than 500 micron. That has been attributed to limited control over pore size and interconnectivity. Therefore, cells that colonise the

periphery of the scaffold, act as a barrier for a deeper diffusion of oxygen and nutrients, thus preventing new cells migrating from further (Sachlos and Czernuszka, 2003).

Traditional TE scaffold manufacturing processes attempt to control the micro-architecture of a scaffold, using a variation of the process parameters. These techniques are limited in their resolution and reproducibility. They might generate a wide distribution of pore sizes but they have poor control over interconnection, geometry, and spatial distribution- things that are essential for the production of regenerated tissue (Taboas *et al.*, 2003).

The use of LM techniques to create TE scaffolds has many advantages. Such technologies allow the realisation of implants with customized external shape via combination with reverse engineered CT or MRI data. Reproducible internal structures are obtainable, giving full control over distribution, interconnection, porosity and channel geometry. That enables an increased and controlled flow inside the scaffold, and therefore aids the regeneration of new tissue. In addition they are cost effective since their manufacture does not involve the production of tooling—thereby allowing the realisation of customised implants.

1.1 Bone Structure

The optimum geometry for TE scaffolds for bone should be similar to that of the native tissue in need of repair. (Lin *et al.*, 2004). TE scaffolds should mimic the structures of both the trabecular (spongy) and cortical (dense) sections of bone. In order to assess and analyse these microstructures, several studies have been conducted using non-destructive techniques--such as Micro-Computed Tomography (μ CT)--that are capable of acquiring images of small bone samples with resolutions of 1 μ m (Genant *et al.*, 1999).

Jones *et al.*, (2004) used μ CT to analyze the morphology and interconnectivity of the regenerated tissue into a polymer scaffold. The Haversian network within a human femoral cortical bone, was rendered into 3D, exposing a very complex system of interconnected channels, as shown in Fig. 1.



Fig. 1 3D rendering of Haversian network in human femoral cortical bone (Jones *et al.*, 2004).

Downey and Siegel (1996) reported the use of μ CT to reconstruct 3D images of iliac crest bone biopsy samples, in order to illustrate change in bone structure due to osteoporosis. The 3D images are shown in Fig. 2.

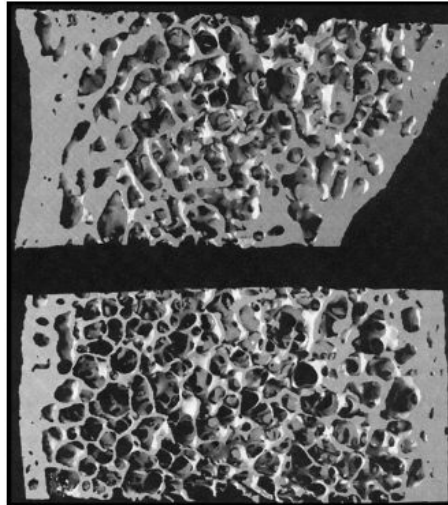


Fig. 2 3D images of iliac crest trabecular bone from the same patient. Top: at age 53. Bottom: at age 58 (Downey and Siegel, 1996).

Das *et al.* (2003) used μ CT derived architecture of a human femur trabecular bone as the basis for creating bio-mimetic scaffolds in Nylon-6. Fig. 3 shows a volumetric rendering of human trabecular bone μ CT data, along with a faceted representation appropriate for use in LM apparatus.

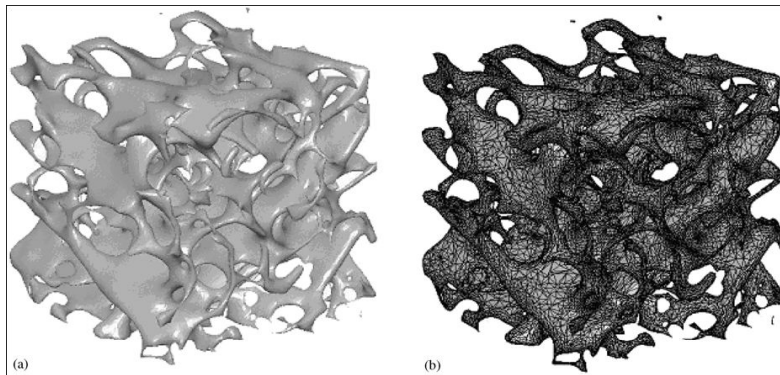


Fig. 3 Volumetric rendering of a human trabecular bone from μ CT (a) and STL representation for layer manufacturing fabrication (b) (Das *et al.*, 2003).

1.2 Scaffold Requirements

There are several optimal requirements for scaffolds. In particular they need: (1) high porosity and interconnecting pores of appropriate size and curvature. The optimal architecture should mimic that of the original tissue; (2) bio-materials with controlled degradation and resorbability rates; (3) adequate mechanical properties for load-bearing applications; (4) a tailored external shape to fit anatomical defects and (5) they must be easily to manufacture and have reproducible internal structures.

While there have been many works on the physical aspects of these requirements, there has been comparatively little investment that considers the design requirements of these highly complex geometries.

Most previous research for the design of TE scaffolds for LM has relied on libraries of unit cells, each with a different, predefined and generally regular internal architecture that does not mimic the natural, highly irregular, structure of bones. Furthermore, the use of unit cells allows control only over the size of some geometrical elements, not their shape, which leads to more regular structures. The selected unit cell is then repeated in 3D to form a prism that contains the entire implant. Using Boolean operations, these two geometries are then combined to design a scaffold with the external shape of the implantation site and the predefined internal structure. Interesting examples of similar approaches can be found in Chua *et al.* (2003), Das and Hollister (2003), Naing *et al.* (2005), Hutmacher *et al.* (2001), Rosen *et al.* (2006).

1.3 Advantages of Automated CAD Design

The aim of this work was to focus attention on an efficient CAD methodology, in order to rapidly enable the design and integration of an intricate network of channels as dictated by a set of variable parameters. The input data can be changed either randomly, or according to given mathematical functions, leading to infinite different networks. The methodology of the work is based on a combination of Object Oriented Programming and CAD software. That allows the design to be produced automatically within a few minutes, featuring a complex and irregular network of channels within any shaped implant, and thereby removes the need to spend innumerable hours attempting to manually model the same architectures. The output data should consist of a standard CAD file of reasonable size that can easily be converted into an STL format for manufacturing by LM.

2. Methodology

Defining a network of channels involves the use of many geometrical parameters including: cross-sections of each channel, its number, size, shape and 3D path. Different algorithms and functions are needed to design these geometries. Those could be routines to perform different tasks such as generating parametric 2D and 3D complex curves, controlling their tangents and curvature, creating points by coordinates and on surfaces, offset and tangent planes, solids and holes of variable cross section, sketches, 2D and 3D constraints, or other functions used to set their location in the space.

In order to test the feasibility of automated design by CAD, several different case studies have been investigated. These examples exhibit a progressive increase in geometry variables and a subsequent complexity related to an increasing number of design functions and routines in accordance with the input data set by the user. The efficiency of such routines is assessed by the output data including computational time and resources, and the resultant file size.

The examples consisted of a small cube (10x10x10 mm) comprised of differently oriented channels of various shapes and sizes. There was no particular requirement to use a cubic shape - any other reference geometry could have been used, but this example provided a regular volume to direct attention onto other parameters, aside from the location of each channel. All the structures reported in this work have a regular location and therefore the position of all channels is fixed. That means that the networks obtained here are irregular in terms of geometry, but not in terms of position. The location of each channel constitutes a parameter which, like all other parameters, can be changed either randomly or according to any mathematical function. However, that was not considered in this section of work since it was not required to assess the proposed methodology. In a future work, the parameter will be changed in different ways, in order to define irregular distributions.

In this work, all input parameters have been changed randomly, each within a user defined range, in order to increase the irregularity of the geometry and to simulate foam structures obtained by scaffolds made using conventional manufacturing techniques.

All the structures shown here were designed using the CAD software Catia® V5 in conjunction with our programme routines and a standard Intel® Pentium® M processor 1.60 MHz laptop, with 752 MB of RAM. A standard computer has been used in this work to pursue novel automated design of TE scaffolds using standard equipment, without the need for high performance computers.

The scaffolds consist of a group of open channels. In order to aid visualisation and understanding of each network, their complementary shape, formed by a network of rods, was also shown. These structures aim to represent the theoretical shape of the regenerated tissue, assuming no degradation of the scaffold.

2.1 Evaluation of Pore Size

In order to simulate an irregular shape in the cross section of each channel, closed 2D splines, consisting of 4 control points, were used. Each control point was positioned as a vertex of a square and, in the first approximation, an estimation of all pore sizes was made, based on the side of each square and its area. The actual porosity is greater than this value, and can be computed using the mathematical formulation of Catia's spline curves. However, throughout this work the pore size was estimated using the above mentioned technique, because a more precise computation does not affect the design methodology itself. Fig. 4 gives an example of how the algorithm for generating such 2D splines works. The estimated pore size is defined by the highlighted square, while the actual size is the area enclosed by the spline. It is, of course, possible to define any other design layout--for example by using a different number of control points in which the coordinates do not necessarily form the vertex of a square, but can be changed randomly in different ranges. It is also possible to control the wall thickness between two consecutive holes either by setting the minimum and maximum, and changing the value as an active constraint on a 2D sketch, or, by introducing other parameters such as the curvature on each control point, accessible in Catia's Application Programming Interface (API). The presented layout was chosen for its simplicity.

STEPS TO CONTROL PORE SIZE AND SHAPE:

- Set pore size range (example 0.2 to 0.8 mm)
- Generation of a random number within this range (0.15 mm in this example)
- Creation of 5 control points (1st and 5th coincident and equal tangent) positioned as 4 vertices of an ideal square
- To obtain different shapes, the tangents are altered

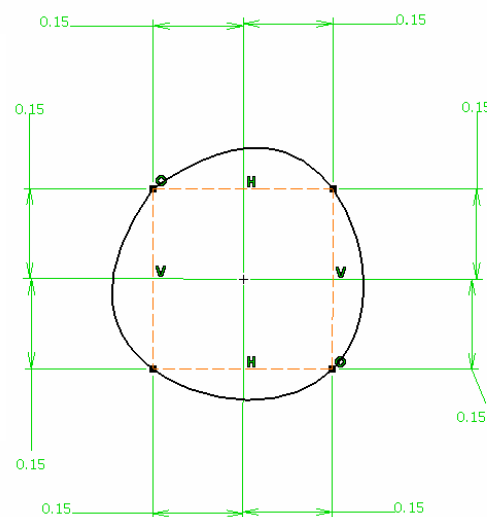


Fig. 4 Steps for creating different porosity and shape in the 2D cross sections of each channel.

3. Results

3.1 Case 1

This case presents a 10 mm cube with a regular distribution of holes of different shapes, obtained by randomly changing the value of the tangents at the control points as parameters. The pore-size range was set from 0.2 mm to 0.8 mm, but the actual pore size is slightly greater, since it was estimated by taking into consideration the square area formed by the 4 control points, which define the profile of each cross section. The pore size range chosen is suitable for regenerating bony tissue (Hulbert *et al.*, 1970). The scaffold is illustrated in Fig. 5 (a), and its negative geometry in Fig. 5 (b). The details of this case are reported in Table 1.

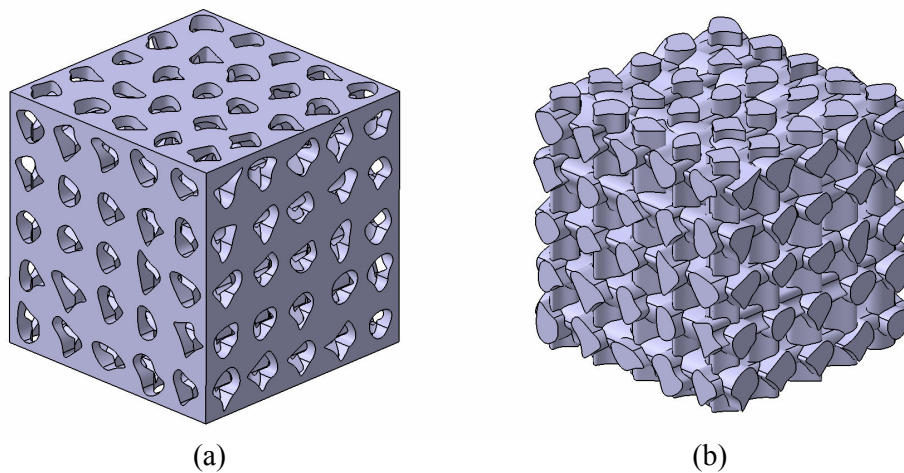


Fig. 5 Case 1: (a) scaffold, (b) theoretical regenerated bone.

	Input Parameters:	Value
Constants	Cube side	10 mm
	Pore size	Range set from 0.2 to 0.8 mm
	Location of holes	Regularly fixed
	Number of holes	5
Variables	Tangents at 4 control points	Random
	Output Parameters:	Value
	Computational Time	13 mins
	Porosity	55.27%
	File size	10.7 MB
	STL size	9.95 MB

Table 1 Case 1: main design and computational data.

3.2 Case 2

This case presents a 10 mm cube with a regular distribution of channels, defined by closed splines and with a step gradient in the cross sections. In each direction and for each hole, the shape changes randomly every 2 mm, by randomly altering the tangents at the 4 control points. The scaffold and its negative shape are illustrated in Fig. 6 (a) and (b) respectively.

Pore size range was set from 0.2 mm to 0.8 mm, considering the approximation of the square area formed by the 4 control points. Fig. 7 shows the step changes in the cross sections in more detail. The details of this case are reported in Table 2.

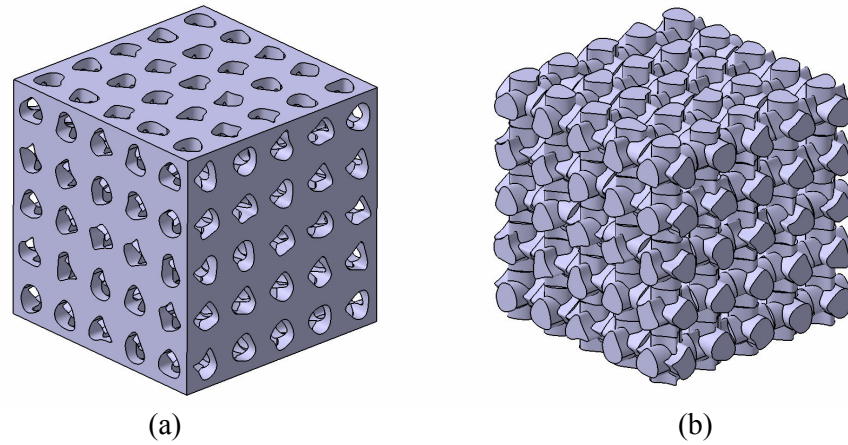


Fig. 6 Case 2: (a) scaffold, (b) theoretical regenerated bone.

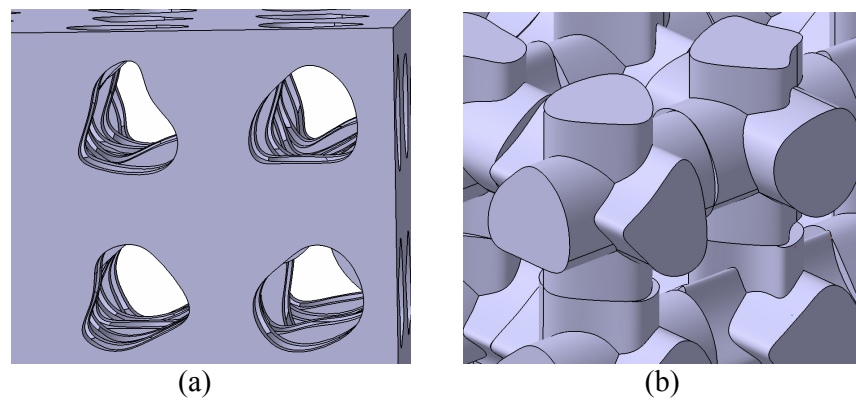


Fig. 7 Case 2: More details of the step changes of the cross sections for: (a) scaffold, (b) theoretical regenerated bone.

	Input Parameters:	Value
Constants	Cube side	10 mm
	Pore size	Range set from 0.2 to 0.8 mm
	Location of holes	Regularly fixed
	Number of holes	5
	Step distance	2 mm
Variables	Tangents at 4 control points	Random x 5 sections
	Output Parameters:	Value
	Computational Time	15 mins
	Porosity	49.95%
	File size	15 MB
	STL size	16.9 MB

Table 2 Case 2: main design and computational data.

3.3 Case 3

This case shows a 10 mm cube with a regular distribution of straight and non-orthogonal channels with 2 cross sections, formed by 2D closed curves (splines with 4 control points). The linear path of each channel is defined by randomly connecting 2 different central points, located on opposite faces.

The shape changes randomly by controlling the tangents at the control points. The scaffold and its negative shape are illustrated in Figs 8 (a) and (b) respectively. Pore size range was set from 0.2 mm to 0.8 mm, with a slightly greater actual size. Fig. 9 shows the linear channels in greater detail.

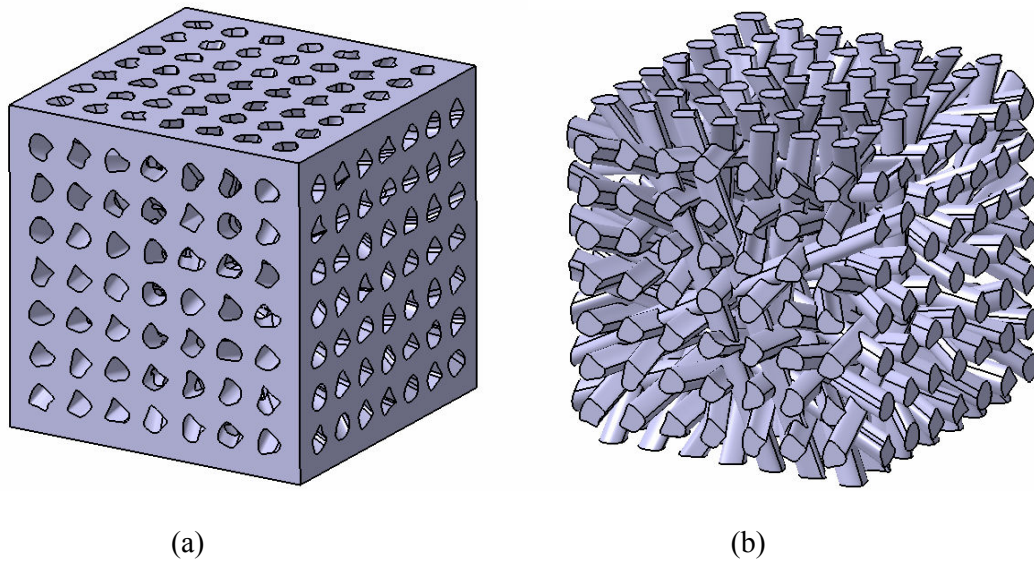


Fig. 8 Case 3: (a) scaffold, (b) theoretical regenerated bone.

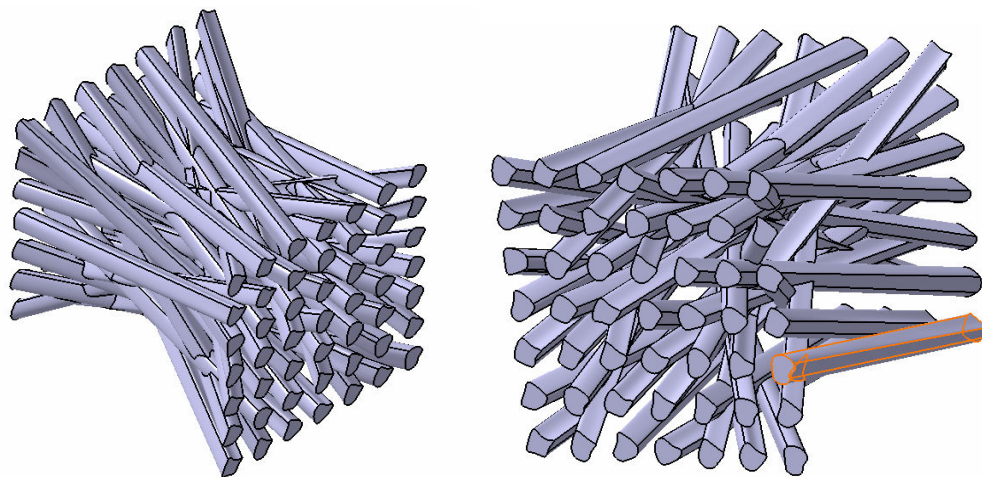


Fig. 9 Case 3: More detail of some linear channels and changes in the cross sections.

The details of this case are reported in Table 3.

	Input Parameters:	Value
Constants	Cube side	10 mm
	Pore size	Range set from 0.2 to 0.8 mm
	Location of holes	Regularly fixed
	Number of holes	7
Variables	Linear path for each channel	Random association of the central points of 2 cross sections in opposite planes
	Tangents at 4 control points	Random x 2 sections
	Output Parameters:	Value
	Computational Time	20 mins
	Porosity	44.16%
	File size	35.7 MB
	STL size	17.4 MB

Table 3 Case 3: main design and computational data.

3.4 Case 4

This case consists of a network of channels made from two cross sections that are both defined by 2D closed splines. Tangents at the four control points are controlled randomly and a 3D spline defines a curved path. As seen previously, there are many different ways to define a pattern and those presented in this and in subsequent cases are simplified solutions since any other arrangement could be set. In this example, all channels were set to converge at the geometrical centre of the cube, in order to improve the porosity and pore interconnectivity of the structure at the scaffold centre, thus mimicking biological internal bone structures (Fig. 10). This design could improve the flow of oxygen, cells and nutrients inside the scaffold and therefore influence the penetration depth of the new tissue, which can be problematic in linear foam scaffold structures.

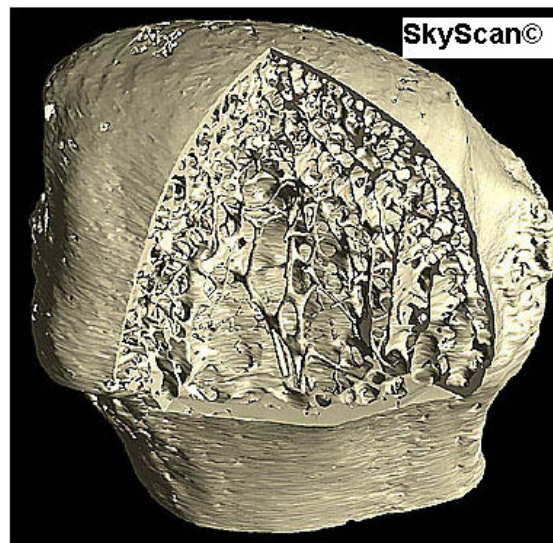


Fig. 10 Example of Metatarsal head μ CT scan, illustrating internal bone structure.

The curved path of each channel is defined by randomly connecting two different 2D curves at the same control points, with a 3D curve through the cube centre. During this process, it is

possible that errors such as twisted and sharp geometries or cusps could cause the end of the programme and interrupt the automated design. To combat this, a routine was specifically designed to detect runtime errors and correct the geometry. This routine automatically detected any error in the geometry, and altered some input parameters until it produced an error-free geometry, without any manual intervention. The user can dictate which parameters are to be changed by such a routine. The tangents at the control points were set by default as was, subsequently, the pore size. That procedure increased computational time because of its need to calculate many different combinations of parameters in order to find a suitable one. Its advantage, however, is that it allowed the automated design of more complex channels involving curvature and 3D paths, along with multi-section elements.

The scaffold and its negative shape are illustrated in Figs 11 (a) and (b) respectively. Again, the pore size range was set from 0.2 mm to 0.8 mm, with a slightly greater actual size. Fig. 12 shows some curved paths and their convergence to the scaffold centre in more detail.

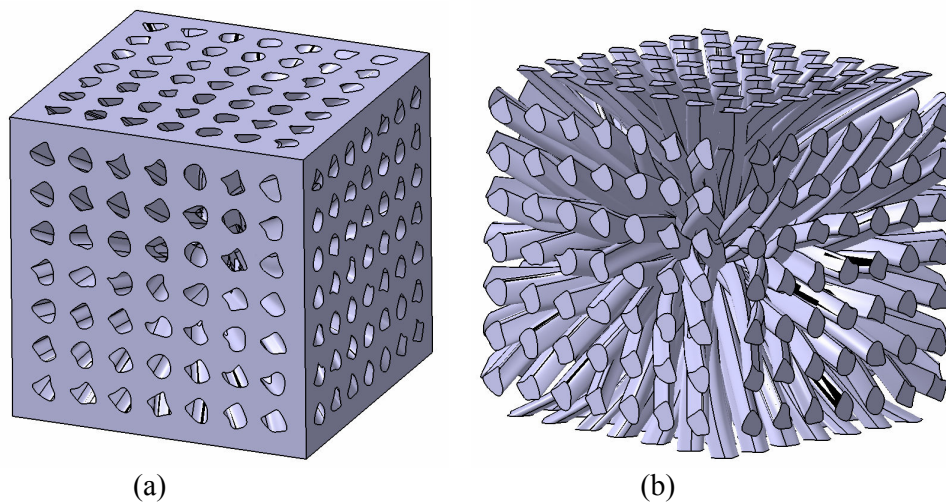


Fig. 11 Case 4: (a) scaffold, (b) theoretical regenerated bone.

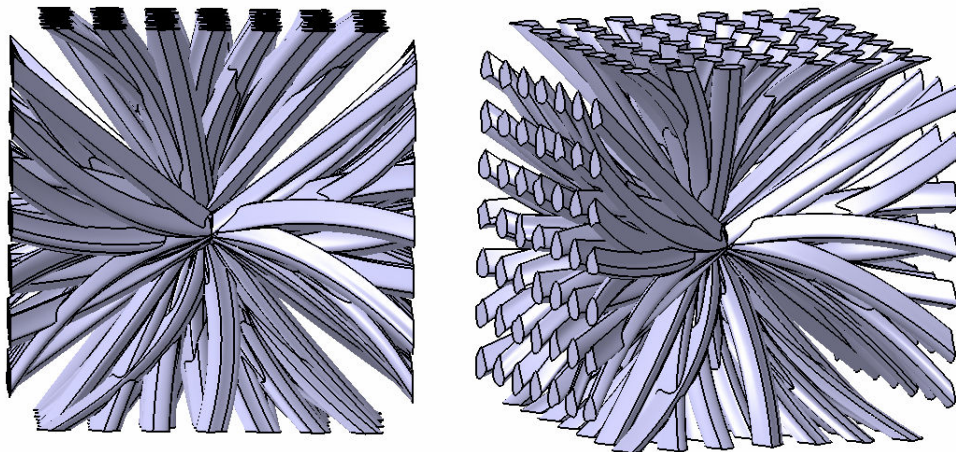


Fig. 12 Case 4: More detail of some curved paths and their convergence to the scaffold centre.

The details of this case are reported in Table 4.

	Input Parameters:	Value
Constants	Cube side	10 mm
	Pore size	Range set from 0.2 to 0.8 mm
	Location of holes	Regularly fixed
	Number of holes	7
Variables	Curved path for each channel	Random association of the central points of 2 cross sections in opposite planes, connected by a 3D curve through the centre
	Tangents at 4 control points	Random x 2 sections
	Output Parameters:	Value
	Computational Time	20 mins
	Porosity	33.56%
	File size	20.6 MB
	STL size	13.6 MB

Table 4 Case 4: main design and computational data.

3.5 Case 5

This case is similar to case 4, although the network is arranged differently. In this example, the channels no longer converge towards the centre, and instead, their path is set randomly in a predefined range. The 3D spline that defines a singular channel is made of three points, the first and third of which are in the two cross sections, and correspond to two control points. The coordinates of the middle point are randomly variable within a range, dictated by user input. Here we have defined a range of $\pm 20\%$ the length of the cube, which means ± 2 mm in each direction in respect to the cube centre. However, any other value could be imposed. As in the previous case, it was necessary to include a routine to detect errors and automatically correct the geometry. The parameters modified by the routine were the tangents at the control points of the 2D splines and the pore size.

The scaffold and its negative shape are illustrated in Figs. 13 (a) and (b) respectively. Pore size range was set from 0.2 mm to 0.8 mm, but again the actual size is slightly greater. Fig. 14 shows some curved paths and their random connections in more detail.

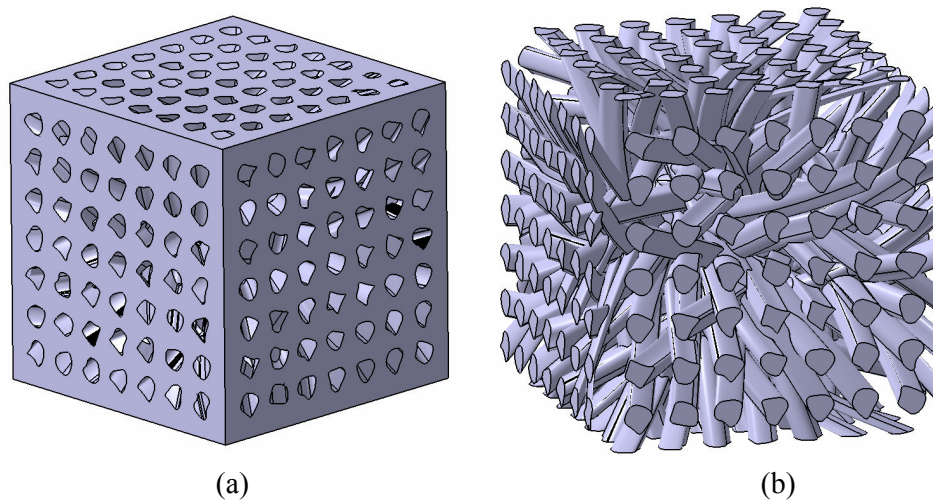


Fig. 13 Case 5: (a) scaffold, (b) theoretical regenerated bone.

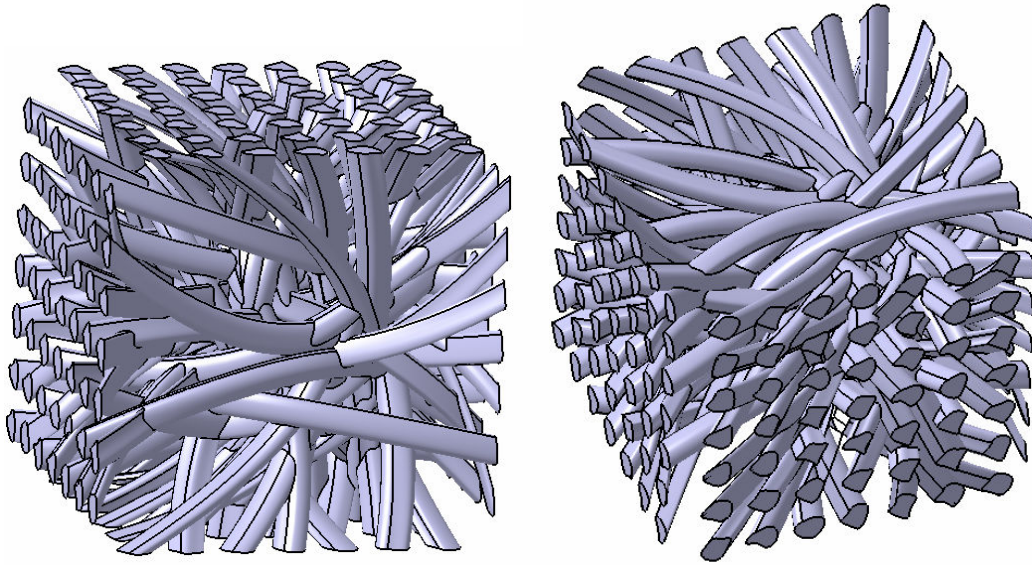


Fig. 14 Case 5: More detail of some curved paths and their random connections.

The details of this case are reported in Table 5.

	Input Parameters:	Value
Constants	Cube side	10 mm
	Pore size	Range set from 0.2 to 0.8 mm
	Location of holes	Regularly fixed
	Number of holes	7
	Control point of the 2 cross sections to be connected by the 3D curve	Fixed
	Ideal Central Volume	$\pm 20\%$ the length of the cube in each direction
Variables	Curved path for each channel	Random association of the central points of 2 cross sections in opposite planes, connected by a 3D curve through a random point within the Ideal Central Volume
	Tangents at 4 control points	Random x 2 sections
	Output Parameters:	Value
	Computational Time	22 mins
	Porosity	36.77%
	File size	35.5 MB
	STL size	24 MB

Table 5 Case 5: main design and computational data.

4. Discussion

The experimental cases have shown that it is possible to achieve the automated design of regular distributions of irregularly and randomly connected channels using CAD software that supports full access to their modelling commands, through API functions such as CatiaV5.

When compared to manual design, the advantages in terms of time are evident. The presented cubes are relatively small, but they could be extended to correspond to the size of a generic implant. The bigger the scaffold, the greater the time that can be saved by using automated design as compared to manual design. Fig. 15 shows the Case 4 scaffold extended to the size of 51 x 41 x 9 mm in order to fit the size of a craniofacial implant. It comprises a regular distribution of 420 channels in the *XY* plane, with each channel having two cross sections. Trying to manually model such a network would be an extremely time consuming task, since for each channel, the user would need to find random combinations of parameters that do not lead to cusps, twists and other errors in the geometry, which may occur frequently in such features. In this case, the design time required by this methodology was 30 minutes, resulting in a CAD file size of 78.8 MB.

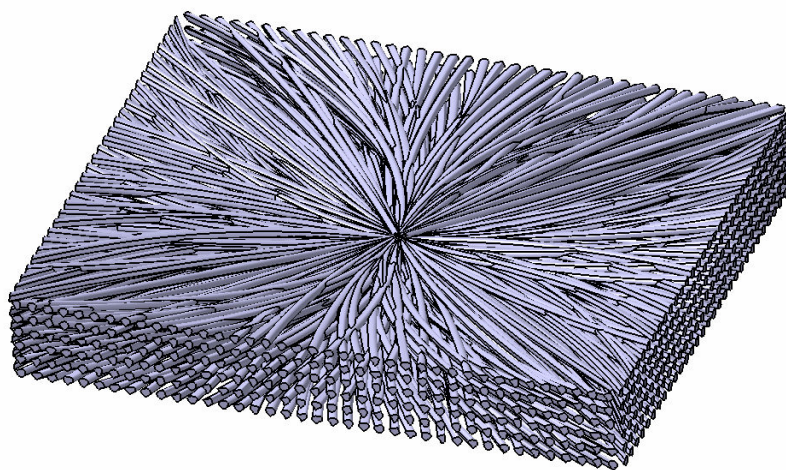


Fig. 15 Example of Case 4 extended to fit the size of an external implant.

However, the advantages of the methodology proposed in this work do not consist purely in time savings, although those are extremely significant. This process could also permit a study of the influence of specific geometric parameters on tissue regeneration—such as the shape of channels and curvature by parametric studies, should all the geometries be fully controllable and reproducible by a layer manufacturing system. The values of all the random parameters can easily be stored in external files and used, for example, as input to redesign similar structures. Furthermore, instead of a random change, any mathematical function can be set for all or some of the inputs, in order to mimic the different densities found in bone structures. The possibilities to further develop this methodology are infinite and overcome the lack of flexibility and the rigid schemes generally encountered in CAD software. The flexibility and versatility of this methodology permits easy adaptation and modification, seen, for example, when the requirements for scaffolds are better defined.

5. Conclusions

Some factors are not incorporated into this methodology. The geometrical design features of the progressive case studies focus on the defined biological requirements identified in other works. It does not fully consider the computation of the mechanical properties of scaffolds, as this was not the purpose of this study. There is also a need for a more precise computation of the pore size and the definition of a parameter to measure pore interconnectivity. The level of

porosity is not yet set as an input parameter, but it is a consequence of the automated design process itself. To adopt that as a direct input, further investigations on the influence of the present input parameters on its resultant value are required.

Ongoing work is being conducted on an efficient and optimised methodology for merging such networks of channels with a generic anatomical geometry from CT scan data, avoiding any Boolean operations. In addition, another class of networks, based on the irregular distribution of irregular channels is being investigated. In these networks, the location of each pore is considered as a random parameter and the connections between two cross sections are no longer located on opposite faces of the cube, resulting in random connections of the six faces. The final distribution of the channels within the cube will therefore be irregular.

Finally, all the input parameters of each case study will be further varied according to different mathematical formulae, in order to try to mimic the natural gradients of density found in bone structures.

References

- Capito, R. M., and M. Spector. 2003. Scaffold-based articular cartilage repair. *IEEE Engineering in Medicine and Biology Magazine* 22, (5): 42-Oct.
- Chua, C. K., K. F. Leong, C. M. Cheah, and S. W. Chua. 2003. Development of a tissue engineering scaffold structure library for rapid prototyping. Investigation and classification. *International Journal of Advanced Manufacturing Technology* 21, (4): 291-301.
- Das S., and Hollister S. J. Tissue Engineering Scaffolds. 2003. *Encyclopedia of Materials: Science and Technology*; ISBN: 0-08-043152-6: 1-7.
- Downey, P. A., and M. I. Siegel. 2006. Perspectives - bone biology and the clinical implications for osteoporosis. *Physical Therapy*. 86, (1): 77.
- Genant, H. K., C. Gordon, Y. Jiang, T. F. Lang, T. M. Link, and S. Majumdar. 1999. Advanced imaging of bone macro and micro structure. *Bone*; 25, (1):149-152.
- Hulbert S. F., F. A. Young, R. S. Mathews, J. J. Klawitter, C. D. Talbert, F. H. Stelling. 1970. Potential of ceramic materials as permanently implantable skeletal prostheses. *J Biomed Mater Res*; 4(3):433-56.
- Hutmacher, D. W., T. Schantz, I. Zein, K. W. Ng, S. H. Teoh, and K. C. Tan. 2001. Mechanical properties and cell cultural response of polycaprolactone scaffolds designed and fabricated via fused deposition modelling. *Journal of Biomedical Materials Research*. 55, (2): 203.
- Jones, A. C., B. Milthorpe, H. Averdunk, A. Limaye, T. J. Senden, A. Sakellariou, A. P. Sheppard, R. M. Sok, M. A. Knackstedt, and A. Brandwood. 2004. Analysis of 3D bone ingrowth into polymer scaffolds via micro-computed tomography imaging. *Biomaterials* 25, (20): 4947-4954.
- Lin, C. Y., N. Kikuchi, and S. J. Hollister. 2004. A novel method for biomaterial scaffold internal architecture design to match bone elastic properties with desired porosity. *Journal of Biomechanics* 37; (5): 623-636.

- Mironov, V., T. Boland, T. Trusk, G. Forgacs, and R. R. Markwald. 2003. Organ printing: Computer-aided jet-based 3D tissue engineering. *Trends in Biotechnology*. 21, (4): 157.
- Naing, M. W., C. K. Chua, K. F. Leong, and Y. Wang. 2005. Fabrication of customised scaffolds using computer-aided design and rapid prototyping techniques. *Rapid Prototyping Journal*. Vol.11 11, (4): 249.
- Rosen, D. W., S. R. Johnston, H. V. Wang. 2006. Design of a graded cellular structure for an acetabular hip replacement component. *Solid FreeForm Fabrication Symposium*.
- Sachlos, E., and J. T. Czernuszka. 2003. Making Tissue Engineering scaffolds work. Review on the application of Solid Freeform Fabrication technology to the production of Tissue Engineering scaffolds. *European Cells and Materials* 5: 29-40.
- Taboas, J. M., R. D. Maddox, P. H. Krebsbach, and S. J. Hollister. 2003. Indirect Solid Freeform Fabrication of local and global porous, Biomimetic and composite 3-D polymer-ceramic scaffolds. *Biomaterials* 24, (1): 181-194.
- Vacanti, J. P., and R. Langer. 1999. Tissue Engineering: the design and fabrication of living replacement devices for surgical reconstruction and transplantation. *The Lancet*, 354: 32-34.